



## Assessing the design rules of electrideres†

Cite this: *J. Mater. Chem. C*,  
2024, 12, 7766Zhikun Yao,<sup>a</sup> Yanzhen Zhao,<sup>a</sup> Wenjun Zhang <sup>a</sup> and Lee A. Burton <sup>\*b</sup>Received 9th April 2024,  
Accepted 3rd May 2024

DOI: 10.1039/d4tc01468e

rsc.li/materials-c

There are three heuristic criteria commonly used to identify electrideres: an apparent valence of plus one, empty space in the crystal structure and the presence of a strongly electron-donating cation. We evoke and explore these criteria by mapping probable charges to a database of all known materials and isolating around around 4000 compounds that are likely to exhibit an oxidation state of +1. Of these, we identify peaks in off-atom electron density by density functional theory and discuss the validity with which the design rules can be applied to these likely electrideres. In doing so, we recover 4 experimentally confirmed electrideres among 51 candidates identified as potential new electrideres that were not considered previously. All results for each candidate are provided but perhaps of special significance is the material  $\text{Ba}_3\text{AlO}_4$  that has similar composition and chemistry to the stable electrider catalyst  $\text{Ca}_{12}\text{Al}_{14}\text{O}_{32}$ . Overall, we find that the valence and void space rules are surprisingly useful but that there is a breadth of chemistry to electrideres that can be overlooked by considering only alkali and alkali earth metal compounds.

## Introduction

Electrideres are materials in which the electrons detach from the valence shell of ions and reside in the crystal structure, acting as anions.<sup>1,2</sup> Because these anionic electrons are not bound to a nucleus, they are easier to migrate and extract compared to electrons in conventional materials, leading to relatively low work functions and high conductivities.<sup>1,3</sup> These properties are desirable for several important technological applications to which it is expected that electrideres can be successfully applied. For example electron emitters,<sup>4</sup> ion sources,<sup>5</sup> light emitting diodes (LED) devices,<sup>6</sup> nonlinear optical switchers,<sup>7</sup> superconductors,<sup>8</sup> and catalysts,<sup>9,10</sup> for *e.g.* the synthesis of ammonia,<sup>11</sup> are all areas of active investigation for electrideres.

The first reports of anionic electrons were detailed for solutions of alkali metals, however attempts to crystallise these systems with the electron remaining off-atom proved difficult.<sup>12</sup> The first successful solid system containing anionic electrons was an organic complex condensed from such a solution by Dye *et al.* in 1983, and given the name electrider.<sup>13</sup> However, the material was extremely unstable at room temperature. It was not until the first purely inorganic electrider was synthesised around 20 years later, that it was demonstrated that electrideres

could be stable with respect to temperature and pressure.<sup>14</sup> The inorganic electrider was synthesised by chemical treatment of the mineral mayenite ( $12\text{CaO}\cdot 7\text{Al}_2\text{O}_3$ ) to remove the oxygen ions from crystallographic cages, creating  $[\text{Ca}_{24}\text{Al}_{28}\text{O}_{64}]^{4+}(4\text{e}^-)$  often written as  $(\text{C}12\text{A}7:\text{e}^-)$ . This material can be considered a zero-dimensional (0D) electrider,<sup>14</sup> as the anion electrons are trapped in a cavity in the crystal structure. There are also 1D electrideres,<sup>15</sup> where anion electrons are confined in a channel of the structure and 2D electrideres,<sup>16</sup> in which anion electrons reside as layers.

In general, electrideres are expected to meet specific conditions that distinguish them from conventional materials.

First, they must have excess electrons,<sup>17</sup> which can be inferred from the apparent oxidation state of the chemical formula. Second, the material must have free space in which the excess electron can reside, hence the 0D, 1D, 2D nomenclature mentioned earlier. Finally, it must contain a cation from which the excess electron will be pushed into the crystal structure and not recombine. For example,  $\text{Ca}_2\text{N}$  the first compound to be confirmed as 2D electrider material,<sup>16</sup> conforms to all three criteria simultaneously, see Fig. 1.  $\text{Ca}_2\text{N}$  has  $2\text{Ca}^{2+}$  cations which provide 4 electrons and  $1\text{N}^{3-}$  anion which can only accept 3 electrons; thus one electron remains unassigned. Together, the  $[\text{Ca}_2\text{N}]^+\text{e}^-$  system is electroneutral but the chemical formula alone denotes an apparent valence of +1. Secondly, the structure of the  $\text{Ca}_2\text{N}$  is layered allowing space for the anionic electrons between the bonded sheets. And finally, the donor ion calcium is extremely electropositive.

Several screening studies have successfully employed the design principles in seeking known or designing new

<sup>a</sup> International Centre for Quantum and Molecular Structures, Department of Physics, Shanghai University, Shanghai 200444, China

<sup>b</sup> Department of Materials Science and Engineering, The Ilby and Aladar Fleiselman Faculty of Engineering, Tel Aviv University, Ramat Aviv, Tel Aviv 6997801, Israel. E-mail: leeburton@tauex.tau.ac.il

† Electronic supplementary information (ESI) available. See DOI: <https://doi.org/10.1039/d4tc01468e>



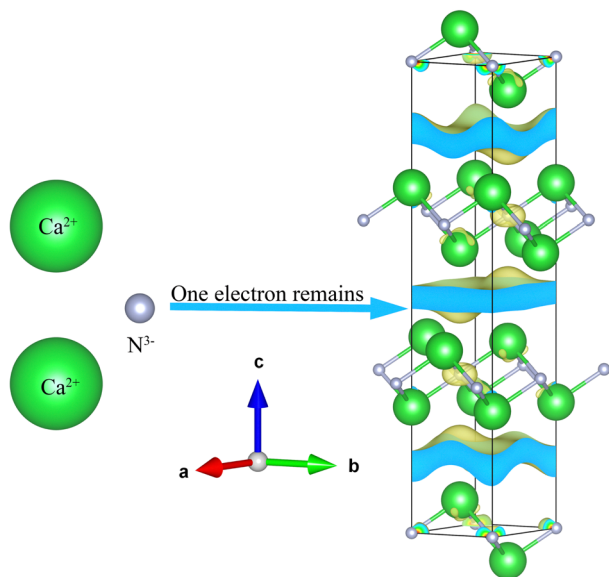


Fig. 1 Illustration of the archetypal electride  $\text{Ca}_2\text{N}$  that conforms to all three heuristic rules of electrides: apparent valence of +1, a crystal void space and an electropositive cation.

electrides.<sup>18–22</sup> However, the degree to which these design principles can be relied upon to define an electride in the general sense has recently been called in to question with the emergence of so-called intermetallic electrides, such as  $\text{La}_3\text{Cu}_2\text{Si}_4$ ,<sup>23</sup>  $\text{Y}_3\text{Pd}_2$ ,<sup>24</sup> and  $\text{LaRuSi}$ <sup>25</sup> reported in the literature. If the design principles are not adhered to, what distinguishes an electride from a metal or mixed alloy? On the other hand, to what extent are the design principles limiting the identification and use of these fascinating systems?

In this paper we investigate the design rules of electrides using a high-throughput approach. We find that the plus one valence rule is a simple yet surprisingly powerful motif in finding and designing new electrides by applying probable valence charge to all stable materials in the Materials Project database. In doing so, we identify 51 candidates as potential new electrides that were not reported previously and are able to use these to further comment on the relevance of the remaining two design principles. Overall, we conclude that electrides encompass a richer and broader swathe of chemistries than was thought possible until now, while confirming the effectiveness of at least two of the existing design rules.

## Methods

The process of high-throughput screening for +1 valence electrides in this work is shown in Fig. 2.<sup>26</sup> Our screening starts from the Materials Project database<sup>27</sup> which includes more than 140 000 inorganic compounds and uses the Vienna ab initio simulation package (VASP) to calculate them.<sup>28</sup> As the definition of electrides requires an excess electron, in the first step, we identify the materials with the total valence as +1, such as  $\text{Ca}_2\text{N}$ . This is accomplished by mapping the most common oxidation states for each element, identified in a previous study,<sup>29</sup> to chemical formulae in the database and summing

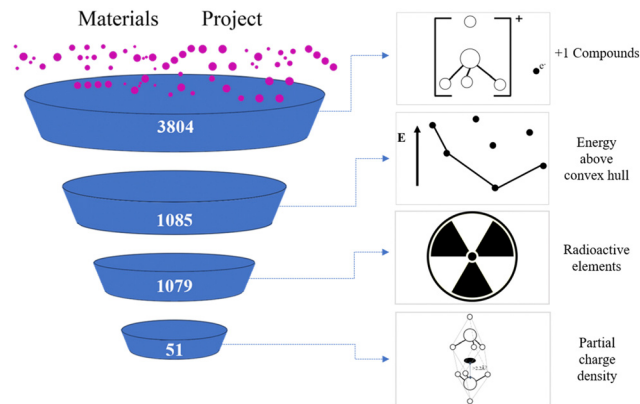


Fig. 2 High-throughput screening process for +1 valence electrides, starting from the Materials Project. The decreasing size of the candidate pools on the left represents the number of compounds remaining after each step elimination process.

the component values. In total this screening provides 3804 candidates.

Subsequently, we eliminate the unstable materials among the plus one valence candidates by cross-referencing the formulae against their “energy above convex hull” parameter in the Materials Project. If the energy is greater than zero eV, the candidates are discarded, leaving 1085 candidates remaining. Then, we also removed any compounds that contain radioactive elements (Np, U, Pa, Th, Pm, Ac) to arrive at a final number of 1079 materials, which were subject to *ab initio* analysis.

*Ab initio* calculations were performed using the Vienna ab initio simulation package (VASP) for the candidates. Density functional theory (DFT)<sup>30</sup> implementing the Perdew–Burke–Ernzerhof (PBE) generalized gradient approximation (GGA) function was used in each case.<sup>31</sup> Spin polarization and magnetism was considered. All VASP input files for the structure optimization were automatically generated by pymatgen<sup>32</sup> “io.vasp.sets” module with the default parameters provided by Materials Project. Bader charge<sup>33–36</sup> analysis was performed to identify the electron distribution of the partial charge density within 0.2 eV around Fermi Energy level. Finally, we use Bader charge analysis to identify maxima in electron density 2.2 Å or more away from the nearest atom. Where present we consider the candidates as electrides, which was found to be effective in this regard in a previous study.<sup>2</sup>

## Results and discussion

The goal of this work is to assess the validity of the three most common design principles for discovering new or uncovering known electrides. Naturally, this goal requires evoking at least one of these design rules first to gain a handle on the electrides against which to benchmark said rules. At the time of writing the Materials Project hosts over 530 000 nanoporous materials, which is a prohibitively large candidate pool and includes families of materials that as yet have produced no confirmed electrides, such as metal–organic-frameworks or MOFs. Thus,



the feature of void space within the crystal structure remains intractable as an early approach to high-throughput analysis for the time being. The heuristic rule of strongly electron-donating constituent elements is one feature to which virtually all confirmed electrified conform and one that could in theory be the starting point for an electrified search. At the time of writing however, there are 60 933 compounds in the Materials Project database containing at least one of the alkali- or alkali-earth metals, which is already unmanageable, without also accounting for electrifieds with cations outside of this group such as the confirmed electrified  $Y_5Si_3$ .<sup>37</sup> By contrast, the rule of total valence summing to plus one has recently become a viable screening tool for the first time. Ding *et al.*<sup>29</sup> reported scanning the inorganic crystal structure database (ICSD)<sup>38</sup> containing 169 800 materials, to find the oxidation states of 108 elements. They found that just 84 oxidation states could cover more than 90% of all reported charges in the ICSD. The small number of the probable oxidation states effectively reduces the combinatorial explosion of possibilities when matching elements to make compounds and allows for a most probably overall valence value to be calculated for a given chemical formula. Fig. 3 is found by taking the most probable oxidation states reported by Ding *et al.* to calculate the overall charge of all compounds in the Materials Project (including those not thermodynamically stable). The x-axis is the total valence of compounds, and the y axis is the number of the compounds corresponding to the total valence. As can be seen, there are around 4000 compounds with an overall oxidation state of +1, which is a surprisingly large candidate pool for finding electrifieds but still much more manageable than the candidates approximated by the other two design rules. Naturally however, the overall largest assigned valence is zero by a wide margin, corroborating the results of the previous study and perhaps explaining the perceived rarity of electrifieds. As for the

compounds that present neither an overall charge of zero or plus one, we see reported entries that have very unique chemistries. For example, the material  $SF_6$  (mp-8560)<sup>39</sup> returns an overall charge of  $-8$  with this method. The large and broad array of materials with charges greater than +1 or indeed greater than +8 predominantly consist of alloys and mixed metals systems, for example  $PuGe_3$  (mp-21484) has a nominative charge of +16 from this approach.<sup>40</sup> We refer the interested reader to the original study of Ding *et al.* for more information,<sup>29</sup> but overall consider these instances as heuristic outliers beyond the scope of this study.

After obtaining the compounds that have an overall valence of +1, an energy above convex hull not greater than 0 eV and no radioactive elements, we simulate the material with density functional theory (DFT). Further analysis using the Bader charge method (described in the Methods section) identifies 51 candidates, which include 4 compounds that have been confirmed as electrifieds previously in experiment ( $Ca_2N$ ,  $Sr_2N$ ,  $Ba_2N$  and  $Ca_{12}Al_{14}O_{32}$ ) and one previously predicted to be an electrified ( $Cs_3O$ ).<sup>41</sup> It is of course unsurprising to find many of the archetypal candidates with the +1 valence design principle, since that principle was derived mainly from these well-known examples, but their presence does lend confidence to the *ab initio* screening approach. The full list of the 51 electrified candidates, their structure and partial charge density can be found in the ESI.†

We conduct analysis on all of the predicted electrified materials that were screened using our method. Firstly, we can consider the design principle of electropositive elements; thus the statistics on the composed elements of these 51 candidates are shown in Fig. 4. The electrifieds are mostly composed of Lanthanide (26.6%) and transition metal (26.6%) elements. For the lanthanides this is perhaps unsurprising as they are relatively electropositive and are unlikely to take back the anionic electron. The prevalence of transition metals is surprising by contrast as transition metals can often present multiple valences and therefore should be able to accept the electron back from the crystal structure. It was only recently that the first redox active electrified was reported with the transition metal chromium in the compound  $Sr_3CrN_3$ .<sup>42</sup> In the  $Sr_3CrN_3$  electrified the Cr exhibits a +4 charge but it is commonly reported as stable at +3, thus it defies expectations by not reclaiming the

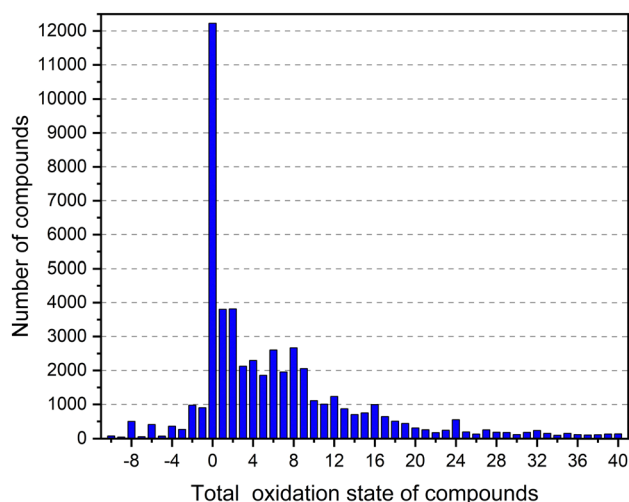


Fig. 3 The distribution of overall oxidation state for compounds in the Materials Project using the most probable valence found by Ding *et al.* The x axis is the total oxidation state of compounds, and the y axis is the number of the compounds corresponding to the total valence.

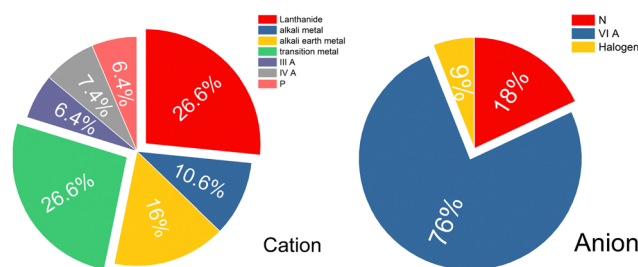


Fig. 4 Percentage distribution of cations (left panel) and anions (right panel) in the identified candidates. The labels IIIA, IVA, P, N, VIA, Halogen correspond to group IIIA elements, group IVA elements, Phosphorus, group VIA elements and Halogens, respectively.



free electron in the crystal structure. Furthermore 16% and 10.6% of electriles are composed of alkali metal and alkali earth metal, respectively, which is a return to expected behaviour in line with existing design principles.

We go further than the usual design rule of only considering the cation to also consider the present anions. For the negatively charged ions, group six elements make up the majority of the composition, accounting for 76%. Such a high prevalence of chalcogenides is quite surprising, especially as oxygen is known to be very electronegative; second only to fluorine in its ability to attract and hold electron density. That said, perhaps the most well-known and well applied electrile is the oxide  $\text{Ca}_{12}\text{Al}_{14}\text{O}_{32}$ . Hopefully this result indicates that yet more air and water stable electriles can be made if the systems are already oxidised in their native form. Only 6% of the total results set is composed of halogens. Halogen electriles have been predicted to exist,<sup>26</sup> but are not prevalent among experimentally demonstrated electriles. It is however, once again not necessarily in line with expectations as a strongly electronegative ion could draw the anionic electron out of the structure. The final surprising result is the relatively small proportion of nitrides among these candidates, considering that nitride compounds comprise the majority of experimentally confirmed electriles. Overall, these findings indicate a surprising breadth to potential electrile chemistry that has barely begun to be accessed, the lanthanide and transition-metal combinations with group VIA elements especially represent a promising but relatively unexplored research area that merits further investigation.

To combine considerations of cation and anion components we consider the general property of electronegativity. Electronegativity is a measure of an atom's ability to attract electrons towards itself when it forms a chemical bond with another atom.<sup>43</sup> We saw that the formation of electriles is often associated with the presence of highly electropositive elements, such as alkali metals, alkaline earth metals, and rare earth metals. These elements have a low electronegativity and can easily donate electrons to form electriles thus it may be the case that chemical formulae with apparent +1 valence also exhibit unusual values in their average electronegativity. The average electronegativity is calculated by multiplying the electronegativity of each element by the corresponding number of atoms in the chemical formula, summing and dividing by the total number of atoms. The average electronegativity of the final 51 candidates can be found in Fig. 5. The full list of all the electronegativities of electriles can be seen in the ESI† (Table S1). As the figure shows, some of the electriles do have a relatively high average electronegativity. For comparison, the materials  $\text{CaCO}_3$ ,  $\text{Fe}_2\text{O}_3$  and  $\text{NaCl}$  have average electronegativities of 1.4, 2.8 and 2.0 respectively and are certainly not considered electriles. However,  $\text{Cs}_3\text{O}$  has the smallest average electronegativity of all candidates of 1.45 and can confidently be counted as an electrile based upon our and other published studies.<sup>41,44</sup> Given that the majority (over 80%) of our candidates have electronegativity values between the 1.4 and 2.8 of the non-electriles  $\text{CaCO}_3$  and  $\text{Fe}_2\text{O}_3$  respectively, it is unlikely

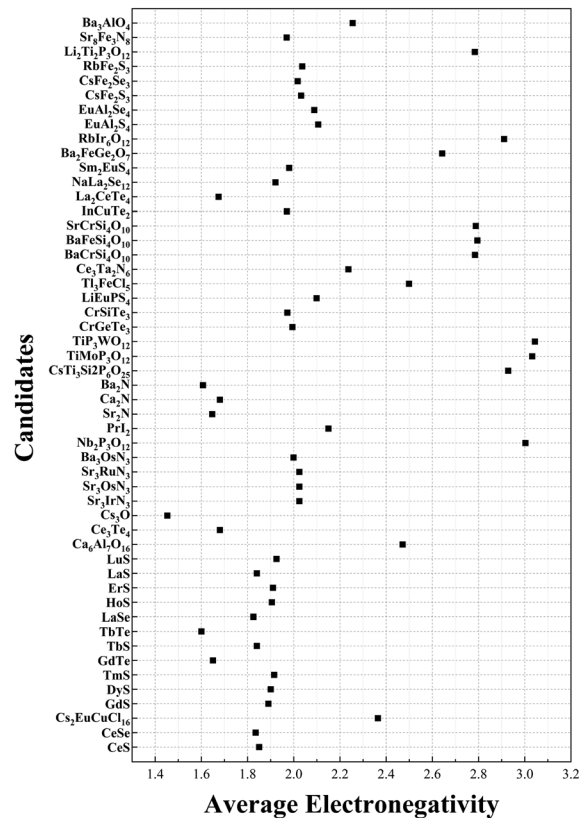


Fig. 5 The average electronegativity for each of the 51 electrile candidates.

that average electronegativity derived from the chemical formula can be used to predict electriles in the same way that total valence appears able.

We also investigate the design principle of internal space for hosting the anionic electron in candidate compounds. In order to assess the influence of internal distance on the identified electriles, we treat the nearest neighbour distance from the off-atom peak in electron density as a variable; the results of which are shown in Fig. 6. The x-axis is the minimum distance we set and the y-axis is the number of candidates containing electron density maxima greater than that distance from the nearest atom. The electrile candidates at each distance are shown in the Table S3 (ESI†). The figure shows the perhaps unsurprising trend that, as the cut-off distance is increased, the number of the candidates decrease quite sharply. However, it is interesting to observe that at 2.8 Å cutoff, all five of the known electriles are present in the 9 candidates alongside  $\text{Sr}_3\text{RuN}_3$ ,  $\text{Sr}_3\text{OsN}_3$ ,  $\text{EuAl}_2\text{S}_4$  and  $\text{Ba}_3\text{AlO}_4$ . In these,  $\text{Sr}_3\text{RuN}_3$  and  $\text{Sr}_3\text{OsN}_3$  have the same prototype structure and consistent formula with the experimentally confirmed electrile  $\text{Sr}_3\text{CrN}_3$  (previously discussed as the first redox active electrile)<sup>42</sup> and  $\text{Ba}_3\text{AlO}_4$  which has a similar composition, component elements and acquisition methods to the confirmed electrile  $\text{Ca}_{12}\text{Al}_{14}\text{O}_{32}$ . Increasing the cutoff further to 2.9 Å results in the three confirmed electriles  $\text{Ca}_2\text{N}$ ,  $\text{Ba}_2\text{N}$ ,  $\text{Ca}_{12}\text{Al}_{14}\text{O}_{32}$  being eliminated among others and leaving the following compounds remaining:



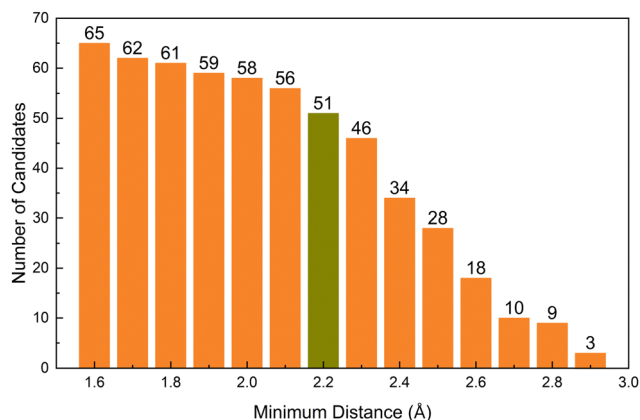


Fig. 6 The number of electrider candidates as a function of minimum distance (in Angstroms) from the nearest atom to the peak in off-atom electron density.

$\text{Sr}_2\text{N}$ ,  $\text{Cs}_3\text{O}$  and  $\text{EuAl}_2\text{S}_4$ .  $\text{Sr}_2\text{N}$  is a previously confirmed electrider,<sup>45</sup>  $\text{Cs}_3\text{O}$  is a previously predicted electrider,<sup>41</sup> but to the knowledge of the authors  $\text{EuAl}_2\text{S}_4$  has not yet been considered as an electrider. Given that every other candidate is all but confirmed to be an electrider we have a high degree of confidence that that  $\text{EuAl}_2\text{S}_4$  will be as well.

The most common structure among the candidates is cubic with space group  $Fm\bar{3}m$  (No. 225). These correspond to  $\text{LaS}$ ,  $\text{LaSe}$ ,  $\text{CeS}$ ,  $\text{CeSe}$ ,  $\text{GdS}$ ,  $\text{GdTe}$ ,  $\text{TbS}$ ,  $\text{DyS}$ ,  $\text{HoS}$ ,  $\text{ErS}$ ,  $\text{TmS}$ ,  $\text{LuS}$ , and  $\text{Cs}_2\text{EuCuCl}_6$ . The anionic electron for these compounds is located in the centre of the cubic coordination environment (see Fig. 7 as an example). Of these 14 cubic systems, 13 are binary compounds composed of f-block elements and group five elements. Those candidates are particularly interesting as they are rare-earth-based electrider, which have been predicted to have high chemical stability and unique electronic properties previously,<sup>46</sup> making them promising candidates for various applications. There are also two candidates that have cubic structure but with the space group  $I\bar{4}3d$  (No. 220), including the first room temperature stable inorganic electrider  $\text{C12A7:e}^-$ ,

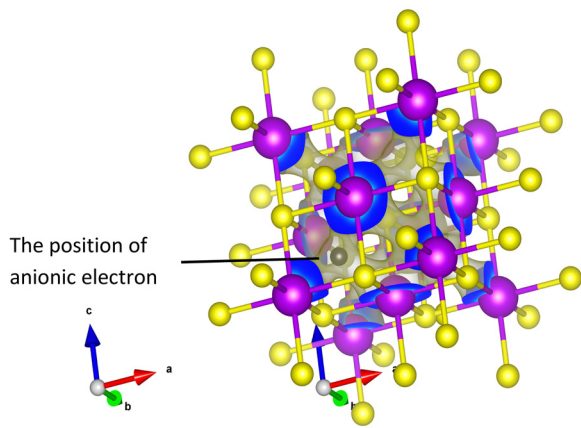


Fig. 7 Electron density around the Fermi level for the material  $\text{CeS}$  as an example of the candidate electrider. The peak in electron density is in the centre of the cubic coordination environment.

which has been well studied before, and the other is  $\text{Ce}_3\text{Te}_4$ . To the knowledge of the authors, it is also the first time for  $\text{Ce}_3\text{Te}_4$  to be considered as an electrider.<sup>47</sup>

In our candidate pool, there are also 4 candidates that match the structure of  $\text{Sr}_3\text{CrN}_3$ , which as mentioned previously was recently reported to be the first electrider with partially filled 3d-shell. These are  $\text{Sr}_3\text{IrN}_3$ ,  $\text{Sr}_3\text{OsN}_3$ ,  $\text{Ba}_3\text{OsN}_3$ ,  $\text{Sr}_3\text{RuN}_3$ , all of them are hexagonal with the space group  $P63/m$  (No. 176). All of them are also ternary transition metal nitride compounds. The anion is located in a one-dimensional (1D) channel formed by a series of oriented cavities throughout the  $c$  axis of the material, see Fig. 8.  $\text{Sr}_3\text{CrN}_3$  itself was found to be an electrider in a previous screening study,<sup>2</sup> however it is not included in our analysis because the oxidation of Cr element in  $\text{Sr}_3\text{CrN}_3$  was allocated as the most common +3 valence in the study of Ding *et al.*, which causes the assigned total valence of  $\text{Sr}_3\text{CrN}_3$  to be equal to zero. However, this result highlights that there is likely a larger family of these 1D electrider compounds either already known or yet to be made and also lends significant credence to the design principle of +1 valence; even after so much research in the area it is possible to find many likely new electrider using such a primitive, heuristic approach.

Additionally, our analysis identifies the interesting candidate  $\text{Ba}_3\text{AlO}_4$ , which derives from the original compound  $\text{Ba}_3\text{AlO}_4\text{H}$ .<sup>48</sup> It has similar composition ratio, component elements and chemistry to  $\text{Ca}_{12}\text{Al}_{14}\text{O}_{32}$  – the first electrider stable at room temperature.  $\text{Ba}_3\text{AlO}_4$  is orthorhombic with the space group  $Pnma$  (No. 62) and is shown alongside  $\text{Ca}_{12}\text{Al}_{14}\text{O}_{32}$  in Fig. 9. Both cases exhibit similar 0D electrider behaviour. We calculate the band structures of  $\text{Ba}_3\text{AlO}_4$  and  $\text{Ba}_3\text{AlO}_4\text{H}$ , as shown in Fig. 10. As we can see, the band gap in  $\text{Ba}_3\text{AlO}_4\text{H}$  disappears in  $\text{Ba}_3\text{AlO}_4$  with the removal of hydrogen atoms, just as is observed for other electrider upon removal of an anion species, *e.g.* H in of  $\text{Sr}_3\text{CrN}_3$  and O in  $\text{Ca}_{12}\text{Al}_{14}\text{O}_{32}$ .<sup>49,50</sup> The bands also show the strongly dispersive nature around the Fermi level, similar to the electronic band structures calculated for other electrider.<sup>2</sup> Finally, while not identical, the analogous compound  $\text{BaAl}_2\text{O}_{4-x}\text{H}_y$  system has been reported as an electrider that can enhance ammonia synthesis when incorporated as a catalyst,<sup>51</sup> again like  $\text{Ca}_{12}\text{Al}_{14}\text{O}_{32}$ ,<sup>11</sup> which boosts the confidence in our findings.

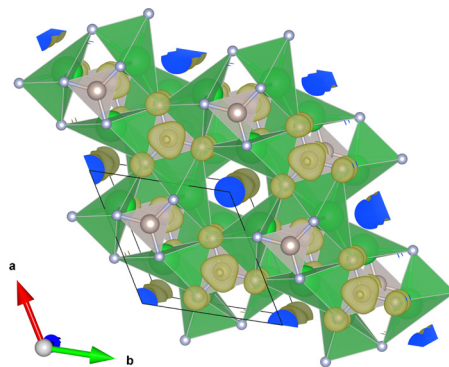


Fig. 8 The electron density channel for the  $\text{Sr}_3\text{CrN}_3$  type compounds ( $\text{Sr}_3\text{RuN}_3$  in this case).



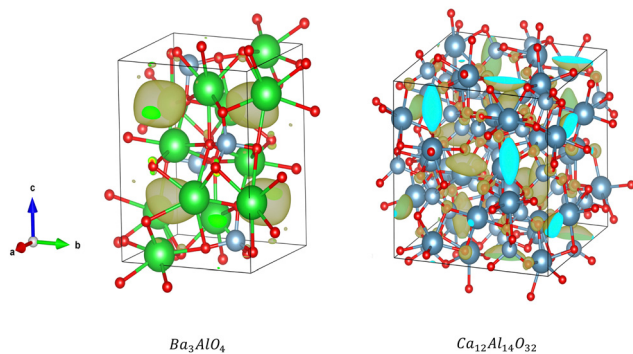


Fig. 9 Electron density around the Fermi level for  $\text{Ba}_3\text{AlO}_4$  (left) and  $\text{Ca}_{12}\text{Al}_{14}\text{O}_{32}$  (right).

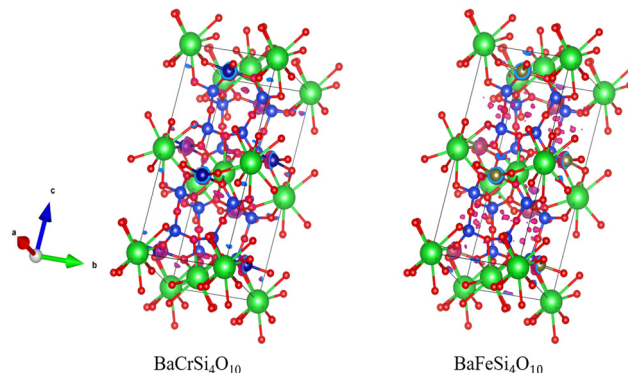


Fig. 11 Electron density around the Fermi level of  $\text{BaCrSi}_4\text{O}_{10}$  (left) and  $\text{BaFeSi}_4\text{O}_{10}$  (right) showing different isosurfaces despite identical chemical structure.

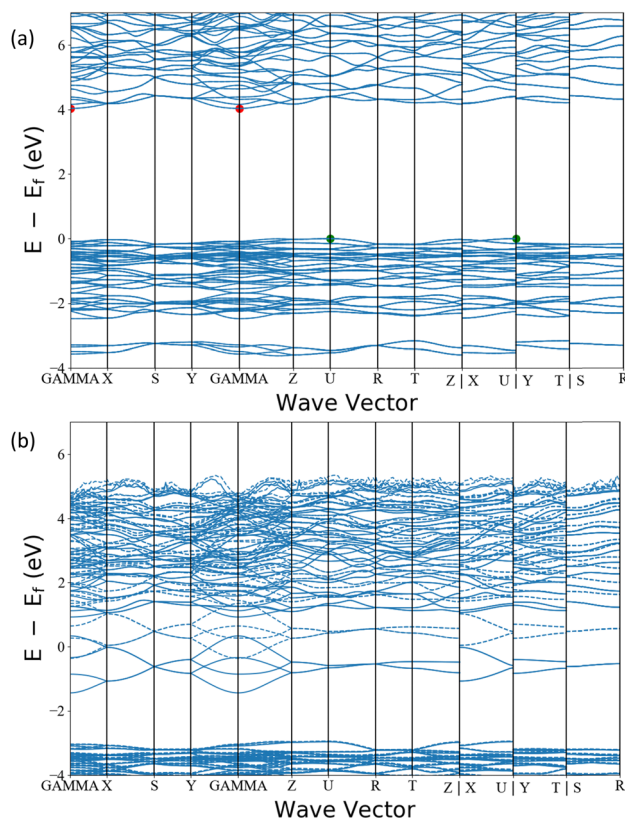


Fig. 10 The electronic band structure of (a)  $\text{Ba}_3\text{AlO}_4\text{H}$  and (b)  $\text{Ba}_3\text{AlO}_4$ .

A few other candidates that are worthy of note are  $\text{Nb}_2\text{P}_3\text{O}_{12}$ , which is the only instance of niobium present in an electride in our candidate set and, to the knowledge of the authors, the first predicted niobium containing electride (see Fig. S17 of the ESI† for the chemical structure and electron density plot for this material). This compound contains no strongly electron positive species, only the niobium, which is of course a transition metal element capable of multiple oxidation states.  $\text{GdS}$  and  $\text{GdTe}$  are also worthy of further exploration as isostructural cubic 0D gadolinium electrides, given that  $\text{Gd}_2\text{C}$  is a known electride that exhibits ferromagnetism above room temperature.<sup>52</sup> The structure and electron density for these compounds is shown in Fig. 7.

In this work and previous works, candidates have tended to be grouped based on their structure. Among the electrides we identified, there are many electrides with same prototype structure and consistent formula, such as  $\text{Sr}_3\text{IrN}_3$ ,  $\text{Sr}_3\text{OsN}_3$ ,  $\text{Sr}_3\text{RuN}_3$ , and  $\text{Ba}_3\text{OsN}_3$ ;  $\text{Ca}_2\text{N}$ ,  $\text{Sr}_2\text{N}$ , and  $\text{Ba}_2\text{N}$ ;  $\text{BaCrSi}_4\text{O}_{10}$ ,  $\text{BaFeSi}_4\text{O}_{10}$  and  $\text{SrCrSi}_4\text{O}_{10}$  *etc.* which indicates that chemical substitution from confirmed electrides is a good way to design new electrides. However, we note that electride behaviour is not solely defined by structure. For instance,  $\text{BaFeSi}_4\text{O}_{10}$  and  $\text{SrCrSi}_4\text{O}_{10}$  are candidates that have the identical structure but have discernibly different electron distributions around the Fermi energy, as show in Fig. 11.

Finally, we highlight potential shortcomings in our method. Firstly, we enforce a criteria of energy above convex hull of 0 eV. This has previously been reported as too strict to account for the errors of DFT and it has previously suggested that a cut-off of 24 meV above convex hull would better capture all candidates instead.<sup>53</sup> Our method also only captures peaks in electron density within a window of 0.2 eV around the Fermi Energy level. This implicitly means that our method will not capture any potential semiconductor electrides, the first of which was reported recently.<sup>54</sup> These drawbacks mean that our results set is likely retrieving the bare minimum candidates and there are many more yet to be uncovered.

## Conclusions

In summary, we have performed a high-throughput *ab initio* screening of all potentially stable electrides by automatically assigning common oxidation states to the constituent elements of compounds that are on their convex hull. Of the >1000 stable materials with a valence of +1 we identify 51 candidate electrides, 4 of which were already proven in experiment-demonstrating the validity of our approach.

We used our results set to effectively explore the established design principles commonly used to identify electrides. We discuss the element composition with respect to cations, anions and overall electronegativity and find a surprising breadth of chemistries on display. The heuristic rule of



necessitating strongly donating cations applies to many cases but not all, see Nb<sub>2</sub>P<sub>3</sub>O<sub>12</sub> for example (Fig. S17, ESI<sup>†</sup>). Similarly, we see a strong presence of transitional metals and variable oxidation state cations in our candidates, see for example CrSiTe<sub>3</sub> (Fig. S27, ESI<sup>†</sup>), which have been previously eschewed in screening studies seeking electrides.<sup>19</sup> We also find that the anions can and are often surprisingly electronegative, with nitrides being a minority of candidates unlike the case for confirmed electrides in experiment. This observation imparts hope for further discovery of more air and water stable electrides such as Ca<sub>12</sub>Al<sub>14</sub>O<sub>32</sub> that can find use in industrial applications. To this end, we recommend the analogous Ba<sub>3</sub>AlO<sub>4</sub> as a promising candidate for future study (Fig. S11, ESI<sup>†</sup>). Unfortunately, we find that average electronegativity does not correlate with electride-like tendencies for compounds.

We also considered the internal space present in the crystal structure of the candidate electrides and find that the design principle of a large pore for hosting anionic electrons appears valid up to a cut-off of around 3 Å. Several of the confirmed electrides conform to this rule at the upper end of the scale. Whether the electrides with this internal distance are disproportionately confirmed in experiment because the largest pore sizes are easier to characterise in experiment or this distance has an intrinsic significance to anionic electron species warrants further investigation.

Finally, our study inherently relies on the design principle of +1 valence. This was a necessity in order to limit the number of candidates to the realm of feasibility but our method of mapping overall valence on to chemical formulae also shows ample positive valence states higher than +1. We believe it likely that more strongly electropositive electrides reside in this space and encourage the exploration of these interesting compounds.

Overall, we believe we have uncovered yet more electrides to contribute to the ever-widening pool of these interesting materials. We have high-confidence in all of our candidates but Ba<sub>3</sub>AlO<sub>4</sub>, Sr<sub>3</sub>IrN<sub>3</sub> and Sr<sub>3</sub>RuN<sub>3</sub> especially are remarkably similar to confirmed electrides.

The compounds discussed in this work are anticipated to have significance for a diverse range of applications and contribute to the fundamental understanding of materials. Each of them are detailed by materials project ID, chemical formula, structure, symmetry and valence electron density in the ESI.<sup>†</sup>

## Conflicts of interest

There are no conflicts to declare.

## References

- C. Liu, S. A. Nikolaev, W. Ren and L. A. Burton, Electrides: A Review, *J. Mater. Chem. C*, 2020, **8**(31), 10551–10567, DOI: [10.1039/D0TC01165G](https://doi.org/10.1039/D0TC01165G).
- L. A. Burton, F. Ricci, W. Chen, G.-M. Rignanesi and G. Hautier, High-Throughput Identification of Electrides from All Known Inorganic Materials, *Chem. Mater.*, 2018, **30**(21), 7521–7526, DOI: [10.1021/acs.chemmater.8b02526](https://doi.org/10.1021/acs.chemmater.8b02526).
- C. Wang, M. Xu, K. T. Butler and L. A. Burton, Ultralow Work Function of the Electride Sr<sub>3</sub>CrN<sub>3</sub>, *Phys. Chem. Chem. Phys.*, 2022, **24**(15), 8854–8858, DOI: [10.1039/D1CP05623A](https://doi.org/10.1039/D1CP05623A).
- R. H. Huang and J. L. Dye, Low Temperature (−80 °C) Thermionic Electron Emission from Alkalides and Electrides, *Chem. Phys. Lett.*, 1990, **166**(2), 133–136, DOI: [10.1016/0009-2614\(90\)87265-S](https://doi.org/10.1016/0009-2614(90)87265-S).
- T. Eguchi, M. Sasao, Y. Shimabukuro, F. Ikemoto, M. Kasaki, H. Nakano, K. Tsumori and M. Wada, A Compact Electron Cyclotron Resonance Negative Hydrogen Ion Source for Evaluation of Plasma Electrode Materials, *Rev. Sci. Instrum.*, 2020, **91**(1), 013508, DOI: [10.1063/1.5128610](https://doi.org/10.1063/1.5128610).
- H. Yanagi, K.-B. Kim, I. Koizumi, M. Kikuchi, H. Hiramatsu, M. Miyakawa, T. Kamiya, M. Hirano and H. Hosono, Low Threshold Voltage and Carrier Injection Properties of Inverted Organic Light-Emitting Diodes with [Ca<sub>24</sub>Al<sub>28</sub>O<sub>64</sub>]<sup>4+</sup> (4e<sup>−</sup>) Cathode and Cu<sub>2−x</sub>Se Anode, *J. Phys. Chem. C*, 2009, **113**(42), 18379–18384, DOI: [10.1021/jp906386q](https://doi.org/10.1021/jp906386q).
- H.-M. He, Y. Li, H. Yang, D. Yu, S.-Y. Li, D. Wu, J.-H. Hou, R.-L. Zhong, Z.-J. Zhou, F.-L. Gu, J. M. Luis and Z.-R. Li, Efficient External Electric Field Manipulated Nonlinear Optical Switches of All-Metal Electride Molecules with Infrared Transparency: Nonbonding Electron Transfer Forms an Excess Electron Lone Pair, *J. Phys. Chem. C*, 2017, **121**(1), 958–968, DOI: [10.1021/acs.jpcc.6b11919](https://doi.org/10.1021/acs.jpcc.6b11919).
- H. Hosono, S.-W. Kim, S. Matsuishi, S. Tanaka, A. Miyake, T. Kagayama and K. Shimizu, Superconductivity in Room-Temperature Stable Electride and High-Pressure Phases of Alkali Metals, *Philos. Trans. R. Soc., A*, 2015, **373**(2037), 20140450, DOI: [10.1098/rsta.2014.0450](https://doi.org/10.1098/rsta.2014.0450).
- T.-N. Ye, J. Li, M. Kitano and H. Hosono, Unique Nanocages of 12CaO·7Al<sub>2</sub>O<sub>3</sub> Boost Heterolytic Hydrogen Activation and Selective Hydrogenation of Heteroarenes over Ruthenium Catalyst, *Green Chem.*, 2017, **19**(3), 749–756, DOI: [10.1039/C6GC02782B](https://doi.org/10.1039/C6GC02782B).
- Y. Toda, H. Hirayama, N. Kuganathan, A. Torrisi, P. V. Sushko and H. Hosono, Activation and Splitting of Carbon Dioxide on the Surface of an Inorganic Electride Material, *Nat. Commun.*, 2013, **4**(1), 2378, DOI: [10.1038/ncomms3378](https://doi.org/10.1038/ncomms3378).
- M. Kitano, Y. Inoue, Y. Yamazaki, F. Hayashi, S. Kanbara, S. Matsuishi, T. Yokoyama, S.-W. Kim, M. Hara and H. Hosono, Ammonia Synthesis Using a Stable Electride as an Electron Donor and Reversible Hydrogen Store, *Nat. Chem.*, 2012, **4**(11), 934–940, DOI: [10.1038/nchem.1476](https://doi.org/10.1038/nchem.1476).
- J. L. Dye and M. G. DeBacker, Physical and Chemical Properties of Alkalides and Electrides, *Annu. Rev. Phys. Chem.*, 1987, **38**(1), 271–299, DOI: [10.1146/annurev.pc.38.100187.001415](https://doi.org/10.1146/annurev.pc.38.100187.001415).
- A. Ellaboudy, J. L. Dye and P. B. Smith, Cesium 18-Crown-6 Compounds. A Crystalline Ceside and a Crystalline Electride, *J. Am. Chem. Soc.*, 1983, **105**(21), 6490–6491, DOI: [10.1021/ja00359a022](https://doi.org/10.1021/ja00359a022).



- 14 S. Matsuishi, Y. Toda, M. Miyakawa, K. Hayashi, T. Kamiya, M. Hirano, I. Tanaka and H. Hosono, High-Density Electron Anions in a Nanoporous Single Crystal:  $[\text{Ca}_{24}\text{Al}_{28}\text{O}_{64}]^{4+}$  ( $4e^-$ ), *Science*, 2003, **301**(5633), 626–629, DOI: [10.1126/science.1083842](https://doi.org/10.1126/science.1083842).
- 15 Y. Zhang, Z. Xiao, T. Kamiya and H. Hosono, Electron Confinement in Channel Spaces for One-Dimensional Electride, *J. Phys. Chem. Lett.*, 2015, **6**(24), 4966–4971, DOI: [10.1021/acs.jpcclett.5b02283](https://doi.org/10.1021/acs.jpcclett.5b02283).
- 16 K. Lee, S. W. Kim, Y. Toda, S. Matsuishi and H. Hosono, Dicalcium Nitride as a Two-Dimensional Electride with an Anionic Electron Layer, *Nature*, 2013, **494**(7437), 336–340, DOI: [10.1038/nature11812](https://doi.org/10.1038/nature11812).
- 17 J. L. Dye, Electrides: Ionic Salts with Electrons as the Anions, *Science*, 1990, **247**(4943), 663–668, DOI: [10.1126/science.247.4943.663](https://doi.org/10.1126/science.247.4943.663).
- 18 Y. Zhang, H. Wang, Y. Wang, L. Zhang and Y. Ma, Computer-Assisted Inverse Design of Inorganic Electrides, *Phys. Rev. X*, 2017, **7**(1), 011017, DOI: [10.1103/PhysRevX.7.011017](https://doi.org/10.1103/PhysRevX.7.011017).
- 19 T. Tada, S. Takemoto, S. Matsuishi and H. Hosono, High-Throughput Ab Initio Screening for Two-Dimensional Electride Materials, *Inorg. Chem.*, 2014, **53**(19), 10347–10358, DOI: [10.1021/ic501362b](https://doi.org/10.1021/ic501362b).
- 20 C. J. Pickard and R. J. Needs, Dense Low-Coordination Phases of Lithium, *Phys. Rev. Lett.*, 2009, **102**(14), 146401, DOI: [10.1103/PhysRevLett.102.146401](https://doi.org/10.1103/PhysRevLett.102.146401).
- 21 Y. Ma, M. Eremets, A. R. Oganov, Y. Xie, I. Trojan, S. Medvedev, A. O. Lyakhov, M. Valle and V. Prakapenka, Transparent Dense Sodium, *Nature*, 2009, **458**(7235), 182–185, DOI: [10.1038/nature07786](https://doi.org/10.1038/nature07786).
- 22 Z. Wang, Y. Gong, M. L. Evans, Y. Yan, S. Wang, N. Miao, R. Zheng, G.-M. Rignanese and J. Wang, Machine Learning-Accelerated Discovery of A2BC2 Ternary Electrides with Diverse Anionic Electron Densities, *J. Am. Chem. Soc.*, 2023, **145**(48), 26412–26424, DOI: [10.1021/jacs.3c10538](https://doi.org/10.1021/jacs.3c10538).
- 23 T.-N. Ye, Y. Lu, J. Li, T. Nakao, H. Yang, T. Tada, M. Kitano and H. Hosono, Copper-Based Intermetallic Electride Catalyst for Chemoselective Hydrogenation Reactions, *J. Am. Chem. Soc.*, 2017, **139**(47), 17089–17097, DOI: [10.1021/jacs.7b08252](https://doi.org/10.1021/jacs.7b08252).
- 24 T.-N. Ye, Y. Lu, Z. Xiao, J. Li, T. Nakao, H. Abe, Y. Niwa, M. Kitano, T. Tada and H. Hosono, Palladium-Bearing Intermetallic Electride as an Efficient and Stable Catalyst for Suzuki Cross-Coupling Reactions, *Nat. Commun.*, 2019, **10**(1), 1–10, DOI: [10.1038/s41467-019-13679-0](https://doi.org/10.1038/s41467-019-13679-0).
- 25 J. Wu, J. Li, Y. Gong, M. Kitano, T. Inoshita and H. Hosono, Intermetallic Electride Catalyst as a Platform for Ammonia Synthesis, *Angew. Chem., Int. Ed.*, 2019, **58**(3), 825–829, DOI: [10.1002/anie.201812131](https://doi.org/10.1002/anie.201812131).
- 26 J. Zhou, L. Shen, M. Yang, H. Cheng, W. Kong and Y. P. Feng, Discovery of Hidden Classes of Layered Electrides by Extensive High-Throughput Material Screening, *Chem. Mater.*, 2019, **31**(6), 1860–1868, DOI: [10.1021/acs.chemmater.8b03021](https://doi.org/10.1021/acs.chemmater.8b03021).
- 27 A. Jain, S. P. Ong, G. Hautier, W. Chen, W. D. Richards, S. Dacek, S. Cholia, D. Gunter, D. Skinner, G. Ceder and K. A. Persson, Commentary: The Materials Project: A Materials Genome Approach to Accelerating Materials Innovation, *APL Mater.*, 2013, **1**(1), 011002, DOI: [10.1063/1.4812323](https://doi.org/10.1063/1.4812323).
- 28 G. Kresse and J. Furthmüller, Efficient iterative schemes for ab initio total-energy calculations using a plane-wave basis set, *Phys. Rev. B: Condens. Matter Mater. Phys.*, 1996, **54**, 11169(accessed 2021-11-23).
- 29 Y. Ding, Y. Kumagai, F. Oba and L. A. Burton, Data-Mining Element Charges in Inorganic Materials, *J. Phys. Chem. Lett.*, 2020, **11**(19), 8264–8267, DOI: [10.1021/acs.jpcclett.0c02072](https://doi.org/10.1021/acs.jpcclett.0c02072).
- 30 P. Hohenberg and W. Kohn, Inhomogeneous Electron Gas, *Phys. Rev.*, 1964, **136**(3B), B864.
- 31 J. P. Perdew, K. Burke and M. Ernzerhof, Generalized Gradient Approximation Made Simple, *Phys. Rev. Lett.*, 1996, **77**(18), 3865–3868, DOI: [10.1103/PhysRevLett.77.3865](https://doi.org/10.1103/PhysRevLett.77.3865).
- 32 S. P. Ong, W. D. Richards, A. Jain, G. Hautier, M. Kocher, S. Cholia, D. Gunter, V. L. Chevrier, K. A. Persson and G. Ceder, Python Materials Genomics (Pymatgen): A Robust, Open-Source Python Library for Materials Analysis, *Comput. Mater. Sci.*, 2013, **68**, 314–319, DOI: [10.1016/j.commatsci.2012.10.028](https://doi.org/10.1016/j.commatsci.2012.10.028).
- 33 W. Tang, E. Sanville and G. Henkelman, A Grid-Based Bader Analysis Algorithm without Lattice Bias, *J. Phys.: Condens. Matter*, 2009, **21**(8), 084204, DOI: [10.1088/0953-8984/21/8/084204](https://doi.org/10.1088/0953-8984/21/8/084204).
- 34 E. Sanville, S. D. Kenny, R. Smith and G. Henkelman, Improved Grid-Based Algorithm for Bader Charge Allocation, *J. Comput. Chem.*, 2007, **28**(5), 899–908, DOI: [10.1002/jcc.20575](https://doi.org/10.1002/jcc.20575).
- 35 G. Henkelman, A. Arnaldsson and H. Jónsson, A Fast and Robust Algorithm for Bader Decomposition of Charge Density, *Comput. Mater. Sci.*, 2006, **36**(3), 354–360, DOI: [10.1016/j.commatsci.2005.04.010](https://doi.org/10.1016/j.commatsci.2005.04.010).
- 36 M. Yu and D. R. Trinkle, Accurate and Efficient Algorithm for Bader Charge Integration, *J. Chem. Phys.*, 2011, **134**(6), 064111, DOI: [10.1063/1.3553716](https://doi.org/10.1063/1.3553716).
- 37 Y. Lu, J. Li, T. Tada, Y. Toda, S. Ueda, T. Yokoyama, M. Kitano and H. Hosono, Water Durable Electride Y5Si3: Electronic Structure and Catalytic Activity for Ammonia Synthesis, *J. Am. Chem. Soc.*, 2016, **138**(12), 3970–3973, DOI: [10.1021/jacs.6b00124](https://doi.org/10.1021/jacs.6b00124).
- 38 Inorganic Crystal Structure Database – ICSD | FIZ Karlsruhe. <https://www.fiz-karlsruhe.de/de/produkte-und-dienstleistungen/inorganic-crystal-structure-database-icsd> (accessed 2021-11-23).
- 39 J. K. Cockcroft and A. N. Fitch, The solid phases of sulphur hexafluoride by powder neutron diffraction, *Z. Kristallogr. - Cryst. Mater.*, 1988, **184**(1–4), 123–146, DOI: [10.1524/zkri.1988.184.14.123](https://doi.org/10.1524/zkri.1988.184.14.123).
- 40 S. M. Baizae and A. Pourghazi, Structural Stability, Electronic Structure and f Hybridization of PuM3 and Pu3M (M = Ge, Sn, Pb) Intermetallic Compounds, *Phys. Rev. B: Condens. Matter Mater. Phys.*, 2007, **387**(1), 287–291, DOI: [10.1016/j.physb.2006.04.034](https://doi.org/10.1016/j.physb.2006.04.034).
- 41 H. Hosono, Electron Transfer from Support/Promotor to Metal Catalyst: Requirements for Effective Support, *Catal. Lett.*, 2022, **152**(2), 307–314, DOI: [10.1007/s10562-021-03648-y](https://doi.org/10.1007/s10562-021-03648-y).



- 42 P. Chanhom, K. E. Fritz, L. A. Burton, J. Kloppenburg, Y. Filinchuk, A. Senyshyn, M. Wang, Z. Feng, N. Insin, J. Suntivich and G. Hautier, Sr<sub>3</sub>CrN<sub>3</sub>: A New Electride with a Partially Filled d-Shell Transition Metal, *J. Am. Chem. Soc.*, 2019, **141**(27), 10595–10598, DOI: [10.1021/jacs.9b03472](https://doi.org/10.1021/jacs.9b03472).
- 43 L. Pauling, The Nature of the Chemical Bond. IV. The Energy of Single Bonds and the Relative Electronegativity of Atoms, *J. Am. Chem. Soc.*, 1932, **54**(9), 3570–3582, DOI: [10.1021/ja01348a011](https://doi.org/10.1021/ja01348a011).
- 44 C. Park, S. W. Kim and M. Yoon, First-Principles Prediction of New Electrides with Nontrivial Band Topology Based on One-Dimensional Building Blocks, *Phys. Rev. Lett.*, 2018, **120**(2), 026401, DOI: [10.1103/PhysRevLett.120.026401](https://doi.org/10.1103/PhysRevLett.120.026401).
- 45 N. E. Brese and M. O'Keeffe, Synthesis, Crystal Structure, and Physical Properties of Sr<sub>2</sub>N, *J. Solid State Chem.*, 1990, **87**(1), 134–140, DOI: [10.1016/0022-4596\(90\)90074-8](https://doi.org/10.1016/0022-4596(90)90074-8).
- 46 Y. Lu, J. Li, T.-N. Ye, Y. Kobayashi, M. Sasase, M. Kitano and H. Hosono, Synthesis of Rare-Earth-Based Metallic Electride Nanoparticles and Their Catalytic Applications to Selective Hydrogenation and Ammonia Synthesis, *ACS Catal.*, 2018, **8**(12), 11054–11058, DOI: [10.1021/acscatal.8b03743](https://doi.org/10.1021/acscatal.8b03743).
- 47 T. Vo, P. von Allmen, C.-K. Huang, J. Ma, S. Bux and J.-P. Fleurial, Electronic and Thermoelectric Properties of Ce<sub>3</sub>Te<sub>4</sub> and La<sub>3</sub>Te<sub>4</sub> Computed with Density Functional Theory with on-Site Coulomb Interaction Correction, *J. Appl. Phys.*, 2014, **116**(13), 133701, DOI: [10.1063/1.4896670](https://doi.org/10.1063/1.4896670).
- 48 B. Huang and J. D. Corbett, Ba<sub>3</sub>AlO<sub>4</sub>H: Synthesis and Structure of a New Hydrogen-Stabilized Phase, *J. Solid State Chem.*, 1998, **141**(2), 570–575, DOI: [10.1006/jssc.1998.8022](https://doi.org/10.1006/jssc.1998.8022).
- 49 M. Xu, C. Wang, B. J. Morgan and A. Burton, L. Hydride Ion Intercalation and Conduction in the Electride Sr<sub>3</sub>CrN<sub>3</sub>, *J. Mater. Chem. C*, 2022, **10**(17), 6628–6633, DOI: [10.1039/D1TC05850A](https://doi.org/10.1039/D1TC05850A).
- 50 R. P. S. M. Lobo, N. Bontemps, M. I. Bertoni, T. O. Mason, K. R. Poepplmeier, A. J. Freeman, M. S. Park and J. E. Medvedeva, Optical Conductivity of Mayenite: From Insulator to Metal, *J. Phys. Chem. C*, 2015, **119**(16), 8849–8856, DOI: [10.1021/acs.jpcc.5b00736](https://doi.org/10.1021/acs.jpcc.5b00736).
- 51 Y. Jiang, R. Takashima, T. Nakao, M. Miyazaki, Y. Lu, M. Sasase, Y. Niwa, H. Abe, M. Kitano and H. Hosono, Boosted Activity of Cobalt Catalysts for Ammonia Synthesis with BaAl<sub>2</sub>O<sub>4-x</sub>Hy Electrides, *J. Am. Chem. Soc.*, 2023, **145**(19), 10669–10680, DOI: [10.1021/jacs.3c01074](https://doi.org/10.1021/jacs.3c01074).
- 52 S. Y. Lee, J.-Y. Hwang, J. Park, C. N. Nandadasa, Y. Kim, J. Bang, K. Lee, K. H. Lee, Y. Zhang, Y. Ma, H. Hosono, Y. H. Lee, S.-G. Kim and S. W. Kim, Ferromagnetic Quasi-Atomic Electrons in Two-Dimensional Electride, *Nat. Commun.*, 2020, **11**(1), 1526, DOI: [10.1038/s41467-020-15253-5](https://doi.org/10.1038/s41467-020-15253-5).
- 53 G. Hautier, S. P. Ong, A. Jain, C. J. Moore and G. Ceder, Accuracy of Density Functional Theory in Predicting Formation Energies of Ternary Oxides from Binary Oxides and Its Implication on Phase Stability, *Phys. Rev. B: Condens. Matter Mater. Phys.*, 2012, **85**(15), 155208, DOI: [10.1103/PhysRevB.85.155208](https://doi.org/10.1103/PhysRevB.85.155208).
- 54 L. M. McRae, R. C. Radomsky, J. T. Pawlik, D. L. Druffel, J. D. Sundberg, M. G. Lanetti, C. L. Donley, K. L. White and S. C. Warren, Sc<sub>2</sub>C, a 2D Semiconducting Electride, *J. Am. Chem. Soc.*, 2022, **144**(24), 10862–10869, DOI: [10.1021/jacs.2c03024](https://doi.org/10.1021/jacs.2c03024).

